

# Analysis of Electronic Structures of Nitrogen $\delta$ -Doped GaAs Superlattices for High Efficiency Intermediate Band Solar Cells

Shunsuke Noguchi, Shuhei Yagi, Daisuke Sato, Yasuto Hijikata, Kentaro Onabe, Shigeyuki Kuboya, and Hiroyuki Yaguchi

**Abstract**—Nitrogen  $\delta$ -doped GaAs superlattices (SLs) were fabricated, and their energy structures were investigated. A number of strong transition signals are observed in photoreflectance (PR) spectra in an energy range from 1.54 to 1.78 eV for SL samples in which any transitions are not observed in uniformly nitrogen-doped GaAsN with comparable nitrogen content. Both of the  $E_+$  and  $E_-$  bands formed around the nitrogen  $\delta$ -doped layers compose SL potentials with the conduction band of the spacer GaAs layers, resulting in the formation of multiple minibands. The energy range of the SL minibands well explains the observed transition energies in the PR spectra. The PR signal intensity ratios of the  $E_+$ -related transitions to the  $E_-$ -related transitions for the SLs are notably large compared with those usually observed for conventional GaAsN alloys. This enhancement of electron transition associated with the  $E_+$ -related bands should be advantageous as intermediate band material. Therefore, nitrogen  $\delta$ -doped GaAs SLs are expected to be an excellent alternative to uniformly doped GaAsN alloys for the use in intermediate band solar cells.

**Index Terms**—Nanostructures, solar energy, spectroscopy, superlattices, III–V semiconductor materials..

## I. INTRODUCTION

MANY novel attempts have been made to improve the efficiency of solar cells in recent years. The intermediate band solar cell (IBSC) [1] is one such attempt. Intermediate band structures can be realized by introducing an allowed state in the forbidden band of semiconductors, which enables below-bandgap photon absorption. The maximum efficiency of the IBSC is theoretically estimated to be more than 63% [1].

GaAsN alloy attracts much attention as one of candidates for the intermediate band material. Alloying up to a few percent

of nitrogen (N) into GaAs leads to the fundamental bandgap reduction. In addition, the existence of an energy band, whose energy is higher than the conduction band (CB) edge of GaAsN and increases with increasing N concentration, was experimentally indicated by means of modulation spectroscopy [2]–[5]. The new energy band formed by N addition is called  $E_+$  band, while the original CB of GaAsN is called  $E_-$  band. Since these  $E_+$ ,  $E_-$ , and the valence bands (VB) are expected to constitute an intermediate band structure, the application of GaAsN to intermediate band solar cells has been studied [6]–[8]. However, in general, the optical transition associated with the  $E_+$  band is not clearly observed compared with the  $E_-$ -VB transition, e.g., the intensity of  $E_+$  transition signals in photoreflectance (PR) and electroreflectance (ER) spectra are usually one tenth or less of that of  $E_-$  transition signals [3]–[5]. It is known that high immiscibility of N into GaAs causes the nonuniform N incorporation into the substitutional sites, thus leading to potential fluctuation at the CB edge [9]–[11]. The  $E_+$  band is possibly more sensitively disturbed by such nonuniformity of N, which results in weak optical transitions. Another explanation may be given by the difference in the localized/delocalized character between the splitting conduction subbands [12]. In any case, in terms of fine formation of intermediate band structures, enhancement of  $E_+$  band transitions in dilute nitride alloys is important. In this study, we propose the use of N  $\delta$ -doped GaAs superlattice (SL) structures as an alternative to uniformly nitrogen-doped GaAsN alloys, and their energy structure is discussed. It is demonstrated that both  $E_+$  and  $E_-$  bands formed around nitrogen  $\delta$ -doped regions compose SL potentials with GaAs CB of spacer regions. Optical transitions attributed to the  $E_+$  band are clearly observed with comparable signal intensity to  $E_-$ -related transitions for such SL structures in PR measurements.

## II. EXPERIMENTAL

Fig. 1 shows a schematic illustration of a sample structure fabricated in this study. The samples were grown by metalorganic vapor phase epitaxy using trimethylgallium, tertiarybutylarsine, and dimethylhydrazine (DMHy) as the Ga, As, and N sources, respectively. A 1000-nm-thick GaAs buffer layer was grown on a GaAs (0 0 1) substrate at 650 °C followed by the growth of a 30-period N  $\delta$ -doped GaAs SL at 570 °C (sample A) or 550 °C (sample B). N  $\delta$ -doped layers were formed by supplying DMHy, while GaAs growth is stopped. The SLs were fabricated by repeating the formation of a  $\delta$ -doped layer and a GaAs

Manuscript received March 8, 2013; revised May 16, 2013; accepted June 24, 2013. Date of publication July 22, 2013; date of current version September 18, 2013. (Corresponding author: S. Yagi.)

S. Noguchi, S. Yagi, Y. Hijikata, and H. Yaguchi are with the Graduate School of Science and Engineering, Saitama University, Saitama, 338-8570, Japan (e-mail: noguchi@opt.ees.saitama-u.ac.jp; yagi@opt.ees.saitama-u.ac.jp; yasuto@opt.ees.saitama-u.ac.jp; yaguchi@opt.ees.saitama-u.ac.jp).

D. Sato is with the Future Project Division, TOYOTA Motor Corporation, Susono, Shizuoka, 410-1193 Japan (e-mail: daisuke@sato.tec.toyota.co.jp).

K. Onabe is with the Department of Advanced Materials Science, The University of Tokyo, Kashiwa, Chiba, 277-8561 Japan (e-mail: onabe@k.u-tokyo.ac.jp).

S. Kuboya is with the Institute for Materials Research, Tohoku University, Sendai, 980-8577 Japan (e-mail: kuboya@imr.tohoku.ac.jp).

Color versions of one or more of the figures in this paper are available online at <http://ieeexplore.ieee.org>.

Digital Object Identifier 10.1109/JPHOTOV.2013.2271978

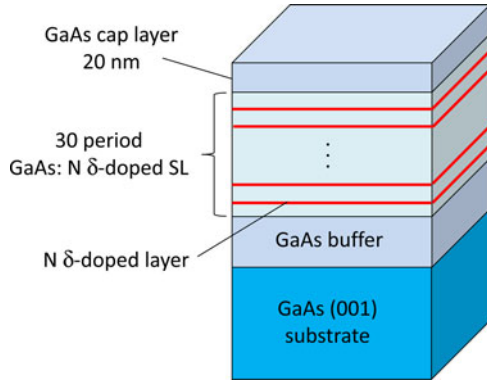


Fig. 1. Schematic illustration of a sample structure with N  $\delta$ -doped GaAs superlattice.

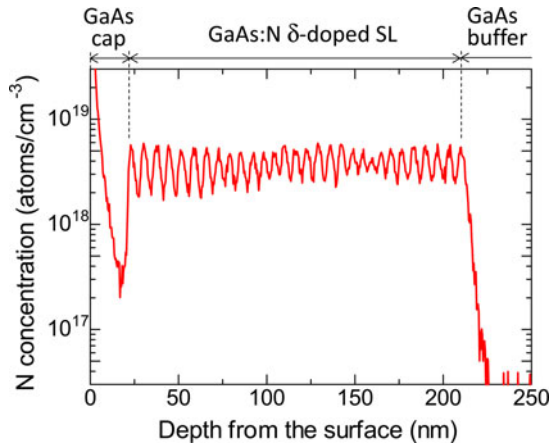


Fig. 2. SIMS profile of N in sample A.

spacer layer, the thickness of which almost corresponding to the SL period. A 20-nm-thick GaAs cap layer was grown on the top of SL. For comparison, a uniformly N-doped GaAsN sample was also prepared. Secondary ion mass spectroscopy (SIMS) was used for the structural evaluation. Photoreflectance (PR) measurements were carried out at 120 K to investigate the energy structures. In the PR measurements, a diode pumped solid-state (DPSS) laser at 532 nm was used as a modulation light. Probe light was illuminated on the surface of the samples by a halogen lamp through a monochromator. PR signals were detected by a Si photodiode using a phase-sensitive lock-in amplification system. Emission properties were characterized by a micro-photoluminescence (PL) system using a DPSS laser (532 nm, 10 mW) as an excitation source.

### III. RESULTS AND DISCUSSION

Fig. 2 shows a SIMS profile of sample A. It is clearly shown that N-doped layers were formed periodically. From the profile, the N area density in a  $\delta$ -doped layer, the SL period and the average N concentration in the SL were estimated. These values are summarized in Table I for both sample A and sample B.

Fig. 3 shows PR spectra of the SL samples. A PR spectrum of a uniformly doped GaAsN with an N concentration of 0.11% is also shown in the figure for comparison. The transition energies

TABLE I  
STRUCTURAL PARAMETERS OF THE FABRICATED NITROGEN  $\delta$ -DOPED SLs  
ESTIMATED FROM SIMS PROFILES

	N area density per layer [cm <sup>-2</sup> ]	Superlattice period [nm]	Average N concentration [%]
sample A	$2.43 \times 10^{12}$	6.46	0.016
sample B	$2.41 \times 10^{13}$	6.88	0.15

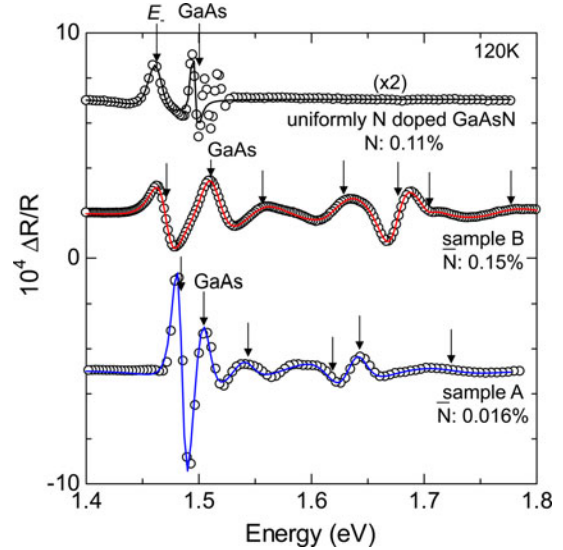


Fig. 3. PR spectra of N  $\delta$ -doped SLs (sample A and sample B) and uniformly doped GaAsN with the N concentration of 0.11% measured at 120 K. The open circles and the solid lines indicate experimental data and fitting curves, respectively. The arrows indicate the obtained transition energy positions by fitting.

were determined by fitting to the Aspnes third-derivative functional form [13], and they are shown by arrows in the figure. GaAs bandgap transition in the cap, buffer layers, or substrates was observed around 1.5 eV in all the samples. Slight difference in the detected GaAs transition energy positions in the spectra is due to a different growth temperature of the GaAs cap layer between the samples. For the uniformly doped GaAsN sample, an oscillatory feature due to the Franz–Keldysh oscillations (FKOs) [14] is observed just above the GaAs bandgap energy. In addition, transitions at energies lower than the GaAs bandgap were observed at 1.485, 1.47, and 1.46 eV for sample A, sample B, and the uniformly doped GaAsN, respectively. These transitions relate to the  $E_-$  bands formed in the N incorporated layers. According to the band anticrossing (BAC) model [2], the  $E_+$  band transition energy of the reference GaAsN (N: 0.11%) sample is expected to be 1.76 eV. However, the  $E_+$  transition is not observable in the spectrum due to its weak signal intensity. On the other hand, only for the SL samples, a number of transitions were clearly observed in the energy range from 1.54 to 1.78 eV in which no transitions are found for uniformly N-doped GaAsN with similar N concentrations as the average value of the SLs. This energy range is in the higher energy side of the GaAs bandgap energy and, simultaneously, is lower than the transition energy usually observed as  $E_+$  band transition in GaAsN alloys. Because the spin-orbit split-off energy of

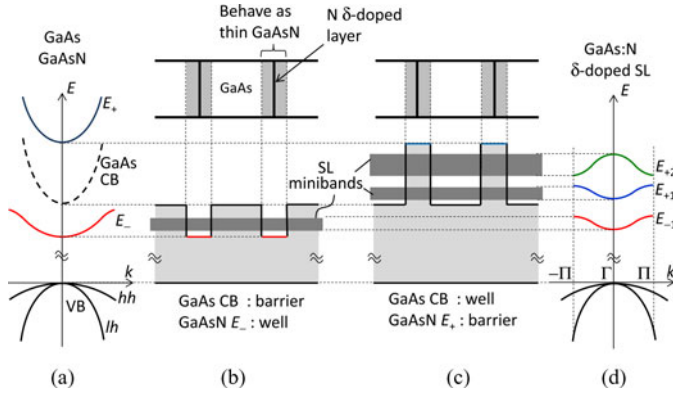


Fig. 4. Schematic illustrations of the energy structure of an N  $\delta$ -doped GaAs SL. The  $E_+$  and  $E_-$  bands are formed around the  $\delta$ -doped layers. These regions are treated as thin GaAs layers with an effective width. (a) Energy dispersion of GaAs and GaAsN (superposed). (b) SL potential consisting of GaAsN  $E_-$  band (well) and GaAs CB (barrier). (c) SL potential consisting of GaAsN  $E_+$  band (barrier) and GaAs CB (well). (d) Energy dispersion of GaAs:N  $\delta$ -doped SL. Minibands are formed by the two sets of SL potentials.

GaAs(N) is 0.33 eV [5], the possibility of the spin-orbit split-off to CB transition can be excluded for the transitions below 1.8 eV. The spectral shapes in the energy range 1.5–1.8 eV for the SLs have considerably different features from the FKOs observed for the uniformly N-doped GaAsN sample which exhibit much smaller oscillation period and gradually attenuated amplitude. Thus, we conclude that the PR signals in the range 1.5–1.8 eV of the SL samples are peculiar to the SL structures. The PR signal intensity ratios of these high energy transitions to the  $E_-$ -band-related transitions are considerably larger than those for usually observed  $E_+$  band transitions in uniformly doped GaAsN alloys, in particular, for sample B.

In order to investigate more details about the origin of these optical transitions, we analyzed the energy structure of N  $\delta$ -doped SLs. Schematic illustrations of the energy structure taken into account in the analysis are shown in Fig. 4. Here, an N  $\delta$ -doped layer is treated as a GaAsN thin layer with an effective width, and thus, the sample is regarded as an SL which consists of GaAs and GaAsN. The CB of the GaAs layers and the  $E_-$  band of the GaAsN thin layers compose a SL potential, and a miniband is formed below the GaAs CB edge. In addition, we assumed that the  $E_+$  band of the GaAsN thin layer and the CB of GaAs also compose a SL potential. In this case, GaAsN and GaAs work as the barrier and the well, respectively, and minibands are formed between the  $E_+$  band edge of GaAsN and the GaAs CB edge.

The energy dispersion of the SL minibands is calculated based on the Krönig–Penny model by changing the effective width and the N composition of GaAsN thin layers while keeping the average N composition in the SL and the SL period. The dependence of the  $E_+$  and  $E_-$  band energies in GaAsN alloys on the N concentration have been widely investigated so far [2]–[5], [15]–[17], and the BAC model is known as a way to describe it [2], [15]. Thus, the bottom energies of  $E_+$  and  $E_-$  bands of the GaAsN thin layer is determined by its dependence expected by the BAC model [2]. The electron effective mass in GaAsN is still controversial. For instance, some experimental

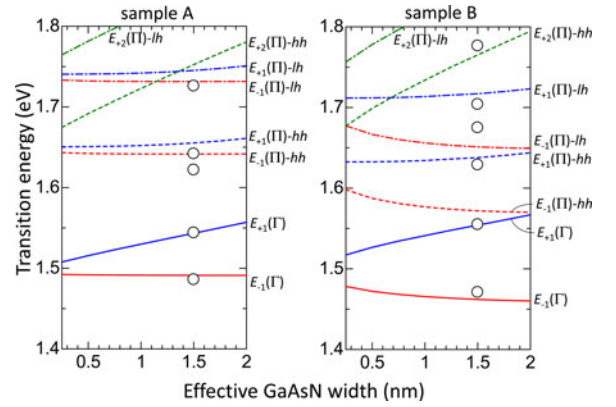


Fig. 5. Dependence of the transition energies on the GaAsN effective width calculated for both (left) sample A and (right) sample B. The notation  $E_{-n}$  ( $E_{+n}$ ) indicates the optical transitions associated with the  $n$ th subband of the  $E_-$  ( $E_+$ )-related SL potential. Transitions at the wavenumber of 0 and  $\pi/l$  ( $l$  is the SL period) are denoted by  $\Gamma$  and  $\Pi$ , respectively. For transitions at the  $\Pi$  point, those associated with heavy hole and light hole are distinguished by the notations hh and lh, respectively. The transition energies taken from the PR spectra are also indicated as open circles, except for the GaAs bandgap transition.

results showed an increase in the effective electron mass in the  $E_-$  band with increasing N content [18], whereas other data suggested the opposite trend [19]. For the  $E_+$  band, there has been no available experimental data on the effective mass. Since the samples prepared in this study contain only small amount of N (the average N content  $<0.2\%$ ), here, we treat the electron effective masses in both the  $E_+$  and  $E_-$  bands as identical with that in the GaAs CB. The VB of the GaAsN thin layers is assumed not to be modulated by N incorporation because the VB offset is much smaller than the CB offset at GaAsN/GaAs interfaces [20], [21]. The energy of optical transitions is estimated from the energy difference between the miniband edges and the VB energy at the corresponding  $k$ -space point. Fig. 5 shows the dependence of the transition energies on the GaAsN effective width calculated for both sample A and sample B. Here, the notation  $E_{-n}$  ( $E_{+n}$ ) indicates the optical transitions associated with the  $n$ th subband of the  $E_-$  ( $E_+$ )-related SL potential. Additionally, transitions at the wavenumber of 0 and  $\pi/l$  ( $l$  is the SL period) are denoted by  $\Gamma$  and  $\Pi$ , respectively. For transitions at the  $\Pi$  point, those associated with heavy hole and light hole are distinguished by the notations hh and lh, respectively. The transition energies taken from the PR spectra are also indicated as open circles in Fig. 5 except for the GaAs bandgap transition. As can be seen in the figure, although slight differences in energy and the absence of observation for a few transitions exist and are probably caused by the simple modeling such as parabolic energy band approximation and rectangular periodic potential, experimentally obtained transition energies are well explained for both the SL samples with different N concentrations if the effective GaAsN width is around 1.5 nm. This fact supports the proposed picture for the energy structure of N  $\delta$ -doped SLs in Fig. 4. Although a part of the observed optical transitions at higher energies than the GaAs bandgap may be due to the  $E_-$ -related transitions at the  $\Pi$  point, more expected transitions related to the  $E_+$  band are found in that energy range.

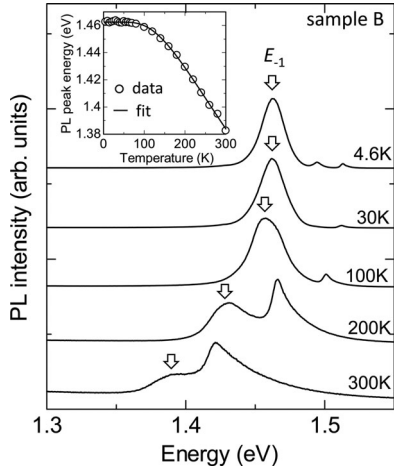


Fig. 6. Normalized PL spectra of sample B measured at 4.6–300 K. The arrows indicate PL peak positions of the  $E_{-1}$  miniband transition in the  $\delta$ -doped SL. The inset indicates the temperature dependence of the PL peak energy of the  $E_{-1}$  miniband transition of the SL. The solid line in the inset is a fitting curve by the Bose–Einstein statistical expression with  $a_B = 0.129$  eV and  $\Theta_B = 433$  K.

Thus, it is reasonable to consider that these high energy transitions mainly originate from the  $E_+$  band formed around the N  $\delta$ -doped layers. As stated previously, the PR signal intensity ratios of the  $E_+$ -related transitions to the  $E_-$ -related transitions for the N  $\delta$ -doped SL samples are notably large compared with those usually observed for conventional GaAsN alloys. This enhancement of electron transition from the  $E_+$ -related bands should be advantageous as intermediate band material. Therefore, N  $\delta$ -doped GaAs SLs are expected to be an excellent alternative to uniformly doped GaAsN alloys for the use in IBSCs.

Fig. 6 shows PL spectra of sample B measured at 4.6–300 K. Emissions at 1.495 and 1.513 eV in the spectrum at 4.6 K are from a localized state related with unintentionally doped carbon impurities and the bandgap transition in the GaAs buffer layer, respectively. The PL peak associated with the  $E_{-1}$  miniband transition in the N  $\delta$ -doped SL is detected at 1.463 eV at 4.6 K. Optical emission by localized carriers on some potential fluctuations due to N incorporation is often dominant in GaAsN alloys at low temperatures. In general, the intensity of PL peak related to the localized states rapidly decreases, and a PL peak due to the GaAsN interband transition, which appears at the higher energy side, becomes dominant with increasing temperature [17], [22]. The inset in Fig. 6 shows the temperature dependence of the PL peak energy of the dominant peak from the N  $\delta$ -doped SL. The PL peak energies are well fitted through the entire temperature range from 4.6 to 300 K by the Bose–Einstein statistical expression [23]

$$E_g(T) = E_g(0) - \frac{2a_B}{\exp(\Theta_B/T) - 1} \quad (1)$$

where  $a_B$  is the electron–phonon interaction strength, and  $\Theta_B$  is the average phonon temperature. The fitting parameters are described in the caption of Fig. 6. This result suggests less potential fluctuation of the miniband edge formed in the SL and

may account for the enhanced signal intensity associated with the  $E_+$  band transitions in the PR spectra.

#### IV. CONCLUSION

We have fabricated N  $\delta$ -doped GaAs SLs and characterized their energy structures. In addition to an electron transition with energy lower than the GaAs bandgap, a number of strong transition signals are observed in the PR spectra in an energy range from 1.54 to 1.78 eV for the SL samples in which no transitions are observed in uniformly N-doped GaAsN with comparable N content. Both of the  $E_+$  and  $E_-$  bands formed around the N  $\delta$ -doped layers compose SL potentials with the CB of the spacer GaAs layers, resulting in the formation of multiple minibands. The energy range of the SL minibands well explains the observed transition energies in the PR spectra. The PR signal intensity ratios of the  $E_+$ -related transitions to the  $E_-$ -related transitions for the SLs are notably large, compared with those usually observed for conventional GaAsN alloys. This enhancement of electron transition associated with the  $E_+$ -related bands should be advantageous as intermediate band material. Therefore, N  $\delta$ -doped GaAs SLs are expected to be an excellent alternative to uniformly doped GaAsN alloys for use in IBSCs.

#### REFERENCES

- [1] A. Luque and A. Martí, “Increasing the efficiency of ideal solar cells by photon induced transitions at intermediate levels,” *Phys. Rev. Lett.*, vol. 78, pp. 5014–5017, 1997.
- [2] W. Shan, W. Walukiewicz, K. M. Yu, J. W. Ager III, E. E. Haller, J. F. Geisz, D. J. Friedman, J. M. Olson, S. R. Kurtz, and C. Nauka, “Effect of nitrogen on the electronic band structure of group III-V-N alloys,” *Phys. Rev. B*, vol. 62, pp. 4211–4214, 2000.
- [3] M. Geddo, T. Ciabattini, G. Guizzetti, M. Patrini, A. Polimeni, R. Trotta, M. Capizzi, G. Bais, M. Piccin, S. Rubini, F. Martelli, and A. Franciosi, “Photoreflectance and reflectance investigation of deuterium-irradiated GaAsN,” *Appl. Phys. Lett.*, vol. 90, pp. 091907–091910, 2007.
- [4] A. Grau, T. Passow, and M. Hetterich, “Temperature dependence of the GaAsN conduction band structure,” *Appl. Phys. Lett.*, vol. 89, pp. 202105–202107, 2006.
- [5] J. D. Perkins, A. Mascarenhas, Y. Zhang, J. F. Geisz, D. J. Friedman, J. M. Olson, and S. R. Kurtz, “Nitrogen-activated transitions, level repulsion, and band gap reduction in GaAs<sub>1-x</sub>N<sub>x</sub> with  $x < 0.03$ ,” *Phys. Rev. Lett.*, vol. 82, pp. 3312–3315, 1999.
- [6] E. Canovas, A. Martí, A. Luque, and W. Walukiewicz, “Optimum nitride concentration in multiband III-V alloys for high efficiency ideal solar cells,” *Appl. Phys. Lett.*, vol. 93, pp. 174109–174111, 2008.
- [7] N. Lopez, L. A. Reichertz, K. M. Yu, K. Campman, and W. Walukiewicz, “Engineering the electronic band structure for multiband solar cells,” *Phys. Rev. Lett.*, vol. 106, pp. 028701–028704, 2011.
- [8] N. Ahsan, N. Miyashita, M. M. Islam, K. M. Yu, W. Walukiewicz, and Y. Okada, “Two-photon excitation in an intermediate band solar cell structure,” *Appl. Phys. Lett.*, vol. 100, pp. 172111–172114, 2012.
- [9] W. Li, M. Pessa, and J. Likonon, “Lattice parameter in GaNAs epilayers on GaAs: Deviation from Vegard’s law,” *Appl. Phys. Lett.*, vol. 78, pp. 2864–2866, 2001.
- [10] W. Li, M. Pessa, T. Ahlgren, and J. Decker, “Origin of improved luminescence efficiency after annealing of Ga(In)NAs materials grown by molecular-beam epitaxy,” *Appl. Phys. Lett.*, vol. 79, pp. 1094–1096, 2001.
- [11] P. R. C. Kent and A. Zunger, “Evolution of III-V nitride alloy electronic structure: The localized to delocalized transition,” *Phys. Rev. Lett.*, vol. 86, pp. 2613–2616, 2001.
- [12] W. Shan, W. Walukiewicz, J. W. Ager III, E. E. Haller, J. F. Geisz, D. J. Friedman, J. M. Olson, and S. R. Kurtz, “Band anticrossing in GaInNAs alloys,” *Phys. Rev. Lett.*, vol. 82, pp. 1221–1224, 1999.
- [13] D. E. Aspnes, “Third-derivative modulation spectroscopy with low-field electroreflectance,” *Surface Sci.*, vol. 37, pp. 418–442, 1973.

- [14] D. E. Aspnes and A. A. Studna, "Schottky-barrier electroreflectance: Application to GaAs," *Phys. Rev. B*, vol. 7, pp. 4605–4625, 1973.
- [15] M. Kondow, K. Uomi, K. Hosomi, and T. Mozume, "Gas-source beam Epitaxy of  $\text{GaN}_x\text{As}_{1-x}$  using a N radical as N source," *Jpn. J. Appl. Phys.*, vol. 33, pp. L1056–L1058, 1994.
- [16] J. Wu, W. Shan, W. Walukiewicz, K. M. Yu, J. W. Ager III, E. E. Haller, H. P. Xin, and W. Tu, "Effect of band anticrossing on the optical transitions in  $\text{GaAs}_{1-x}\text{N}_x/\text{GaAs}$  multiple quantum wells," *Phys. Rev. B*, vol. 64, pp. 085320–085323, 2001.
- [17] H. Yaguchi, S. Kikuchi, Y. Hijikata, S. Yoshida, D. Aoki, and K. Onabe, "Photoluminescence study on temperature dependence of band gap energy of GaAsN alloys," *Phys State Solid b*, vol. 228, pp. 273–277, 2001.
- [18] P. N. Hai, W. M. Chen, I. A. Buyanova, H. P. Xin, and C. W. Tu, "Direct determination of electron effective mass in GaNAs/GaAs quantum wells," *Appl. Phys. Lett.*, vol. 77, pp. 1843–1845, 2000.
- [19] D. L. Young, J. F. Geisz, and T. J. Coutts, "Nitrogen-induced decrease of the electron effective mass in  $\text{GaAs}_{1-x}\text{N}_x$  thin films measured by thermomagnetic transport phenomena," *Appl. Phys. Lett.*, vol. 82, pp. 1236–1238, 2003.
- [20] M. Kozhevnikov, V. Narayanamurti, C. V. Reddy, H. P. Xin, C. W. Tu, A. Mascarenhas, and Y. Zhang, "Evolution of  $\text{GaAs}_{1-x}\text{N}_x$  conduction states and giant Au/ $\text{GaAs}_{1-x}\text{N}_x$  Schottky barrier reduction studied by ballistic electron emission spectroscopy," *Phys. Rev. B*, vol. 61, pp. R7861–R7864, 2000.
- [21] T. Kitatani, M. Kondow, T. Kikawa, Y. Yazawa, M. Okai, and K. Uomi, "Analysis of band offset in GaNAs/GaAs by X-ray photoelectron spectroscopy," *Jpn. J. Appl. Phys.*, vol. 38, pp. 5003–5006, 1999.
- [22] S. Francoeur, S. Anikishin, C. Jin, Y. Qiu, and H. Temkin, "Exciton bound to nitrogen cluster in GaAsN," *Appl. Phys. Lett.*, vol. 75, pp. 1538–1540, 1999.
- [23] L. Vina, S. Logothetidis, and M. Cardona, "Temperature dependence of the dielectric function of germanium," *Phys. Rev. B*, vol. 30, pp. 1979–1991, 1984.

Authors' photographs and biographies not available at the time of publication.